Journal of Catalysis **197,** 49–57 (2001)
doi:10.1006/jcat.2000.3035, available online at http://www.idealibrary.com on IDEAL®

Oligomerization of Ethene In a Slurry Reactor Using a Nickel(II)-Exchanged Silica–Alumina Catalyst

Michael D. Heydenrych,* Christakis P. Nicolaides,† and Michael S. Scurrell‡,[1]

*Department of Chemical Engineering, University of Pretoria, Pretoria 0002, South Africa; †Chemical Process Engineering Research Institute, Centre for Research and Technology—Hellas, P.O. Box 361, 57001 Thermi-Thessaloniki, Greece; and ‡Department of Chemistry, Applied Chemistry and Chemical Technology Centre, University of the Witwatersrand, P.O. Wits, Johannesburg 2050, South Africa

Received April 14, 2000; revised August 15, 2000; accepted August 15, 2000

Ethene oligomerization kinetics on a nickel(II)-exchanged silica–alumina catalyst were determined using a mechanically stirred laboratory-scale slurry reactor. With analysis of both gaseous and liquid outlets from the reactor, the various reaction rates could be correlated in terms of liquid-phase reactant concentrations. In addition, vapour–liquid equilibria could be measured. All experiments were carried out at an operating pressure of 3.5 MPa and the temperature was varied between 120 and 180°C. The feed MHSV was varied between 1 and 12. Three second-order reactions were used to correlate the observed rate of ethene conversion and the Schulz–Flory-type product distribution: ethene–ethene dimerization, ethene–oligomer reaction, and butene–butene dimerization. The inferred rate of butene dimerization was confirmed experimentally using butene as the reactant feed. Very little deactivation was observed during experimental runs lasting 900 h or more, with conversions being maintained throughout at over 90%. Oligomers up to C_{16} were obtained. The absolute rate of ethene oligomerization typically exceeded 11.5 g g_{cat}^{-1} h^{-1}. It was shown experimentally that both gas–liquid and interparticle mass transfer limitations were absent in this work.

Key Words: **ethene oligomerization; slurry reactor; nickel(II)-exchanged silica–alumina; kinetics; rate constants; butene.**

1. INTRODUCTION

The behaviour of catalysts prepared by the ion exchange of nickel(II) onto silica–alumina supports in the oligomerization of ethene has recently been described (1). The essential features of the catalytic system comprise the stable oligomerization of ethene to C_4–C_{20} products at low temperature and high pressure. At 120°C, 3.5 MPa, and MHSV = 2 in a fixed-bed flow reactor, the conversion of ethene typically reaches 97–99% and greater than 97% of the products contain an even number of carbon atoms per molecule. Useful though the fixed-bed system is in establishing the overall behaviour of this catalyst, the high exothermicity of the oligomerization process would render scale-up difficult. In addition, to establish accurate kinetic data, a CSTR reactor configuration is more useful. Therefore, a study of the conversion of ethene using a slurry reactor was undertaken. The primary objectives were to determine the intrinsic kinetics of the oligomerization reaction, the product spectrum that can be obtained, and the stability of the catalyst under slurry reactor operation.

2. EXPERIMENTAL

A stainless steel reactor of nominal internal volume of 700 ml was used. The reactor was approximately half-filled with liquid oligomer produced in a prerun carried out before the actual experimental run was deemed to have commenced. Ethene or butene were fed to the reactor in a controlled manner using a mass flow controller or a positive displacement pump, respectively. An inert gas (usually nitrogen) was used as an internal standard for determining the rate of flow of gaseous products from the reactor. The liquid level in the reactor was determined using a differential pressure transducer and controlled by means of an electrically actuated valve. The level control and the gas and liquid outlets provided for separation of the gaseous and liquid fractions formed under reaction conditions. In this manner, the vapour concentration of reactants in the liquid at the surface of the catalyst could be measured directly to determine the reaction kinetics. In addition, the vapour–liquid equilibrium could also be determined. Analyses of gaseous and liquid products were conducted using gas chromatographic procedures described before (1).

The catalysts used were identical to those described in detail in our previous publication and designated as NiSA-II (1). They were prepared by nickel exchange of the silica–alumina supports with nickel chloride solutions at reflux. After purification (1), the nickel content was 1.6% by mass. The catalyst particle sizes used in the present study are indicated in the text.

[1] To whom correspondence should be addressed. Department of Chemistry, University of the Witwatersrand, Private Bag 3, P.O. Wits, Johannesburg, 2050, South Africa. E-mail: scurrell@aurum.chem.wits.ac.za.

0021-9517/01 $35.00

In a typical experimental run a mass of 9.14 g of catalyst was used and preconditioned for 16 h using a temperature of 250°C with flowing nitrogen. Thereafter, the reactor was cooled to the desired temperature and ethene (or butene) feed was introduced in a gradual manner to avoid any temperature excursions in the reactor. When the liquid level in the reactor (due to oligomer formation) had become measurable, the rate of feed was increased to the desired normal operating flow rate. At the same time the pressure in the reactor was gradually raised to the operating level. Normally, the operating pressure was reached when the reactor was about 20% full. The entire start-up procedure (excluding the catalyst conditioning step) took about 3 h. After 2 or 3 days consistent catalytic performance had usually been achieved and data collection was undertaken. The total pressure in the reactor was maintained at 3.5 MPa throughout. This was identical to the pressure used for the fixed-bed microreactor work that was reported previously (1).

For ethene as feed, overall mass balances were better than 96%. With butene as feed the mass balances were better than 95%.

Oligomerization runs were performed using MHSV values between 2 and 12, with reaction temperatures selected to lie between 120 and 160°C.

3. DESCRIPTION OF THE MODELS EXAMINED

Vapour–Liquid Equilibrium

The vapour–liquid separation obtained with the reactor system was compared with data predicted using the PROCESS software of Simulated Sciences Inc. The K values, defined as the ratio of the molar concentration in the gas phase to the molar concentration in the liquid phase, are compared in Table 1. The SRK vapour–liquid equilibrium model (2) was used in the PROCESS package.

All components heavier than C_{10} were lumped together as a C_{13} species. (The effective chain growth probability, as depicted in Fig. 5, is 0.727 and using this value, the average carbon number of the C_{11}–C_{18} fraction is 12.98.) All the component data were for linear alkenes. Only in the case of octene is there a significant error between measured and predicted values. This is ascribed to the very low concentration of octene found in the gas phase. Overall, the data show very good agreement and vapour–liquid equilibrium values measured in the system are reliable. It therefore appears that the reactor system is free of any effects due to liquid entrainment in the gaseous product lines, and there are also no gas–liquid mass transfer resistances in the system (see below).

TABLE 1

Comparison of K Values for Ethene Oligomerization at 140°C and 3.5 MPa

Component	K (experimental)	K (SRK)	Error %
Nitrogen	12.4404	11.3867	9.2
Ethene	3.4523	3.4108	1.2
Ethane	3.1272	2.8533	9.6
Butene	0.9175	0.8867	3.5
Hexene	0.3814	0.3999	−4.6
Octene	0.1768	0.1291	36.9

Mass Balance

Gas chromatographic analyses were performed as mass fractions for 23 components (alkenes in the range C_2 to C_{20}, nitrogen, methane, ethane, and propane). In practice the concentrations of the alkanes were negligible under the reaction conditions studied. For the purposes of the model presented here all isomeric alkenes of a given C number are lumped together and treated as a single component.

The stream notation used is depicted in Fig. 1. Gas chromatographic analyses gave the mass fractions $z_{B,i}$, $z_{C,i}$, and $z_{D,i}$. The mole fractions of streams B, C, and D are

$$X_i = \frac{z_i/M_i}{\sum z_i/M_i}. \quad [1]$$

The volume flow rate of stream C (Q_C) is determined using a wet gas flowmeter at atmospheric pressure and the ideal gas law was used to calculate the molar flow rate of stream C:

$$X_{C,tot} = Q_C p_{atm}/RT. \quad [2]$$

The mass flow rate of stream C is then given by

$$Z_{C,tot} = x_{C,tot} \sum x_i M_i \quad [3]$$

and the individual component mass flow rates as

$$Z_{C,i} = z_{C,i} Z_{C,tot}. \quad [4]$$

Calculation of Rate Constants

A general model was first derived for the oligomerization of any lower alkene, where products are expressed in terms of multiples of the monomer. This is designated Model 1. An extension of the first model, designated Model 2, is derived particularly for ethene oligomerization to take into account non-zero rates of conversion of the butenes formed. For the well-stirred two-phase reactor system employed in this work applicable mass flows are as shown in Fig. 2. The gas and liquid phases are in equilibrium and products in the gas and liquid phases leave the reactor at volumetric flow rates of Q_G and Q_L, respectively. Mass and molar flow rates are given by Z and X, respectively, and mass and mole fractions are designated z_i and x_i, respectively, where the subscripts denote the stream number and component identity. The gas- and liquid-phase component concentrations in the

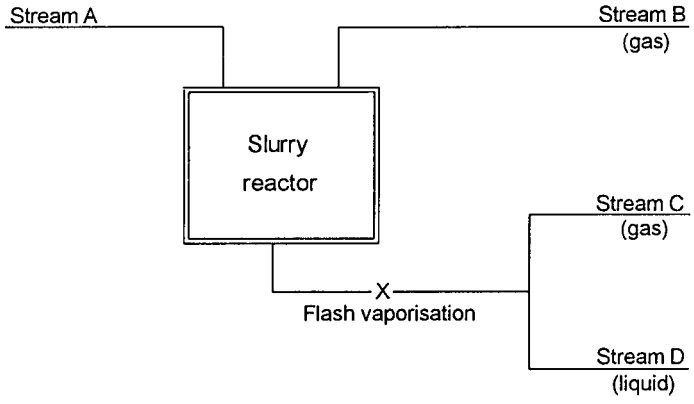

$x_{A,i}$: mole fraction of component i in Stream A

$X_{A,i}$: molar flow rate of i in Stream A

$z_{A,i}$: mass fraction of i in Stream A

$Z_{A,i}$: mass flow rate of i in Stream A

Components are numbered as follows: i=1 represents nitrogen, and i=2 to 20 represents the carbon number of alkene components; alkanes are numbered 21-23

FIG. 1. Stream notation for the mass balance.

reactor $C_{G,i}$ and $C_{L,i}$ are related by the solubility coefficient, m_i:

$$C_{G,i} = m_i C_{L,i}. \quad [5]$$

The mass balance for a single component is

$$F_i + r_i - Q_G m_i C_{L,i} - Q_L C_{L,i} = 0, \quad [1 < i < \infty]. \quad [6]$$

Assuming that the liquid density is essentially independent of composition, for a given volume, the sum of all moles of monomer must equal the mass of liquid divided by the molecular mass of the monomer,

$$\sum_{i=1}^{\infty} i C_{L,i} = \rho_L / M_i, \quad [7]$$

where M_i is the molecular mass of monomer.

For ideal gas behaviour,

$$\sum_{i=1}^{\infty} M_i C_{L,i} = P/RT. \quad [8]$$

For the general case where the rate constant for the reaction between any two species i and j is given by $k_{i,j}$, the rate of formation (i.e., consumption) of the monomer is given by

$$r_1 = -2k_{1,1} w_{cat} (C_{L,i})^2 - w_{cat} C_{L,1} \sum_{i=2}^{\infty} k_{1,i} C_{L,i} \quad [9]$$

and the rate of formation of any other component $[i > 1]$ is given by

$$r_i = w_{cat} \left[\sum_{j=1}^{i/2} k_{j,i-j} C_{L,j} C_{L,i-j} - C_{L,i} \sum_{j=1}^{\infty} k_{i,j} C_{L,j} - k_{i,i} C_{L,i}^2 \right]. \quad [10]$$

(If i is an odd number, the limiting value of the first sum is $[i-1]/2$.) The number of components in this general system is infinite and so too is the number of rate constants.

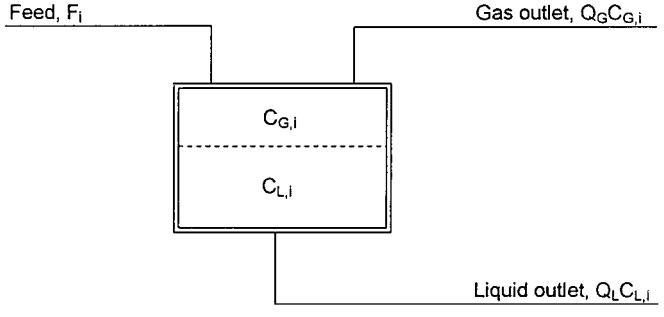

Units : Q in m^3/h

C in kg-mol/m^3

F in kg-mol/h

FIG. 2. Two-phase model reactor.

It is necessary to determine a relationship between the rate constants to determine the concentrations of consecutive oligomers. The two models developed, Model 1 (applicable to butene as the feed) and Model 2 (applicable to ethene as the feed), use two parameters and three parameters, respectively, in describing the rate constants. Each model is reviewed in turn.

Model 1

The following relationships between the rate constants are used as the basis for this model:

$$k_{1,1} = k_1 \quad [11]$$

$$k_{1,i} = k_2 \quad (2 \le i < \infty) \quad [12]$$

$$\text{all other } k_{ij} = 0. \quad [13]$$

The solution of Eq. [6] leads to the following relationship between consecutive oligomers:

$$C_{\mathrm{L},2} = \frac{k_1 w_{\mathrm{cat}} C_{\mathrm{L},1}^2 + F_2}{k_2 w_{\mathrm{cat}} C_{\mathrm{L},1} + Q_{\mathrm{G}} m_2 + Q_{\mathrm{L}}}, \quad (i = 2) \quad [14]$$

$$C_{\mathrm{L},i} = \frac{k_2 w_{\mathrm{cat}} C_{\mathrm{L},1} C_{1,i-1} + F_i}{k_2 w_{\mathrm{cat}} C_{\mathrm{L},1} + Q_{\mathrm{G}} m_i + Q_{\mathrm{L}}}, \quad (i > 2). \quad [15]$$

Note that with only monomer as the feed and when $m = 0$ (large i), a geometric progression in the liquid-phase concentrations of consecutive oligomers is predicted, described by Schulz–Flory product distributions (3). The chain growth probability, α, is defined as

$$\alpha = \frac{k_2 w_{\mathrm{cat}} C_{\mathrm{L},1}}{k_2 w_{\mathrm{cat}} C_{\mathrm{L},1} + Q_{\mathrm{L}}}. \quad [16]$$

The liquid-phase product distribution of this set of reactions (where $m_i = 0$) is shown in Fig. 3. Note that the concentration of any component is dependent entirely on the concentration of the next lightest component.

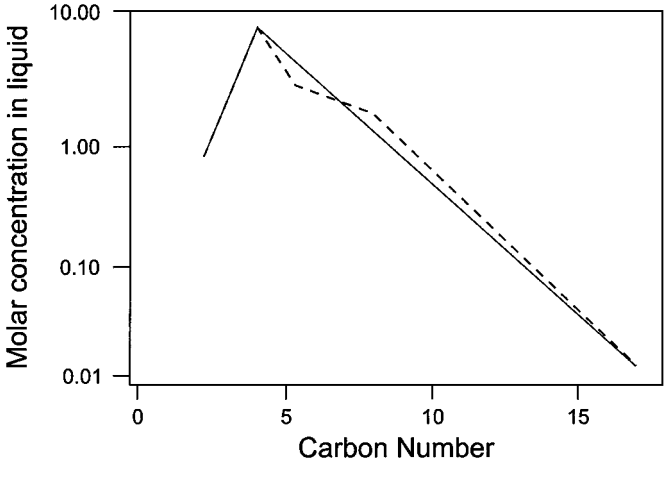

FIG. 3. Product distribution for the two-parameter model 1 — and the three-parameter model 2 - - - for MHSV = 2.

Model 2

When the feed monomer is ethene, the assumption contained in Model 1 that $k_{2,2} = 0$ will not necessarily hold; in other words, a non-zero rate of butene dimerization has to be considered. [In the context of the present work experimental data show that other rate constants $k_{2,i}$ $(i > 2)$ are sufficiently low under all conditions that they can be ignored.] Model 1 is adjusted to incorporate the rate constant $k_{2,2}$:

$$\text{Define} \quad k_{2,2} = k_3. \quad [17]$$

This reaction affects only rates r_2 and r_4. r_2 is calculated as follows:

$$r_2 = w_{\mathrm{cat}} \left[k_1 C_{\mathrm{L},1}^2 - k_2 C_{\mathrm{L},1} C_{\mathrm{L},2} - 2 k_3 C_{\mathrm{L},2}^2 \right]. \quad [18]$$

Solving for $C_{\mathrm{L},2}$,

$$C_{\mathrm{L},2} = \frac{-b \pm \sqrt{b^2 - 4ac}}{2a}, \quad [19]$$

where

$$a = 2 w_{\mathrm{cat}} k_3$$

$$b = k_2 w_{\mathrm{cat}} C_{\mathrm{L},1} + Q_{\mathrm{G}} m_2 + Q_{\mathrm{L}}$$

$$c = -F_2 - k_1 w_{\mathrm{cat}} C_{\mathrm{L},1}^2.$$

(The positive root must be used since both a and b are always positive.)

Similarly,

$$r_4 = w_{\mathrm{cat}} \left[k_2 C_{\mathrm{L},1} C_{\mathrm{L},3} - k_2 C_{\mathrm{L},1} C_{\mathrm{L},4} + k_3 C_{\mathrm{L},2}^2 \right]. \quad [20]$$

And solving for $C_{\mathrm{L},4}$,

$$C_{\mathrm{L},4} = \frac{k_3 w_{\mathrm{cat}} C_{\mathrm{L},2}^2 + k_2 w_{\mathrm{cat}} C_{\mathrm{L},1} C_{\mathrm{L},3} + F_4}{k_2 w_{\mathrm{cat}} C_{\mathrm{L},1} + Q_{\mathrm{G}} m_4 + Q_{\mathrm{L}}}. \quad [21]$$

A typical product distribution obtained with Model 2 is shown in Fig. 3.

4. SOLUTION OF THE REACTOR MODEL

To solve the reactor model, an infinite sum (Eq. [7]) must be evaluated. It has been shown that when the solubility coefficients tend to zero (with higher carbon number products), the product distribution follows a geometric progression. This property of the system can be used to solve Eq. [7]. Note that Eq. [8] is not an infinite sum if, beyond some value of i, the solubility coefficients of all heavier components are considered to be zero.

Assuming that $n-1$ components have solubility coefficients that are sufficiently large enough that they exert an effect on the solution of the model ($n > 4$), Eq. [7] can be written in the form

$$\sum_{i=1}^{n-1} iC_{\mathrm{L},i} + \sum_{i=n}^{\infty} iC_{\mathrm{L},i} = \rho_{\mathrm{L}}/M_i. \qquad [22]$$

The second term can be rewritten in terms of α:

$$\begin{aligned}\sum_{i=n}^{\infty} iC_{\mathrm{L},i} &= nC_{\mathrm{L},n} + (n+1)C_{\mathrm{L},n+1} + (n+2)C_{\mathrm{L},n+2} + \cdots \\ &= C_{\mathrm{L},n}[n + (n+1)\alpha + (n+2)\alpha^2 + \cdots] \\ &= \alpha[n/(1-\alpha) + \alpha/(1-\alpha)^2]C_{n-1}. \qquad [23]\end{aligned}$$

If $C_{\mathrm{L},i}$, Q_{G}, and Q_{L} are known, all concentrations can be determined successively up to $C_{\mathrm{L},n-1}$ using Eqs. [14] and [15] for Model 1 and Eqs. [14], [15], [19], and [20] for Model 2. The solution of $C_{\mathrm{L},1}$, Q_{G}, and Q_{L} must be determined numerically since the equations are nonlinear in these variables.

A Simplex hill-climbing method was used (4). This approach has the advantage of reliability; speed was not particularly important when there were as few as three unknowns.

Solubilities were determined by reference to vapour–liquid equilibrium data. Because of the infinite number of components that needed to be considered in this work, use was made of the homologous nature of the series of alkenes involved in oligomerization processes. A model developed by Caldwell and van Vuuren (5) for predicting the vapour pressures of alkane products obtained via the Fischer–Tropsch (FT) synthesis was used as a basis for the present work. For FT products the vapour pressure of an alkane as a function of temperature and carbon number is predicted by the equation

$$\ln p_i = A - B(1/T - C), \qquad [24]$$

where

$$\begin{aligned}A &= 9.7891 \\ B &= 427.218 \text{ and} \\ C &= 1.029807 \times 10^{-3}.\end{aligned}$$

This correlation originally presented for temperatures in the range 180–400°C was found to require slight modification for the lower temperature range of 80–180°C applicable to the present oligomerization work. The temperature coefficients for lower temperatures then become

$$\begin{aligned}B &= 539.333 \text{ and} \\ C &= 1.2522 \times 10^{-3}.\end{aligned}$$

TABLE 2

Vapour Pressure Correlation and Literature Values

Component	Pressure (kPa)	Temperature (°C)		
		Correlation	Alkane	Alkene
C_{10}	5.32	83.4	85.5	83.3
C_{10}	13.30	106.4	108.6	106.5
C_{10}	53.20	147.5	150.6	149.2
C_{10}	101.08	169.6	174.1	172.0
C_{12}	1.33	89.2	90.0	87.8
C_{12}	5.32	119.7	121.7	118.6
C_{12}	13.30	142.8	146.2	142.3
C_{16}	0.13	104.2	105.3	101.6
C_{16}	1.33	146.5	149.8	146.2
C_{16}	5.32	176.8	181.3	178.8

In addition, for alkenes rather than alkanes it was found that the coefficient A should be increased slightly to 10.042.

Table 2 shows the good agreement between the predicted and literature values for C_{10}, C_{12}, and C_{16} alkenes. Although the temperatures involved may exceed the critical temperatures of the lower alkenes, it is common practice to use hypothetical vapour pressures for the purposes of performing vapour–liquid equilibrium calculations. The model does not provide for vapour–liquid equilibrium for nitrogen, and further, the extension of the model to components as light as butene and ethene necessitates the use of slightly revised Antoine coefficients. The latter were obtained by experimental measurements of solubilities and the values are summarized in Table 3.

Gas-phase concentrations could be calculated as follows:

$$C_{\mathrm{G},i} = \frac{C_{\mathrm{L},i}\, p_i}{\left[\sum_j^{\infty} C_{\mathrm{L},j}\right] RT}. \qquad [25]$$

And the solubilities were then obtained according to the definition of solubility coefficients,

$$m_i = C_{\mathrm{G},i}/C_{\mathrm{L},i}$$

where

$$m_i = \frac{p_i}{\left[\sum_j^{\infty} C_{\mathrm{L},j}\right] RT}. \qquad [26]$$

TABLE 3

Antoine Coefficients Used for Light Components

Component	A	B
Nitrogen	12.9214	−935.83
Ethene	14.0789	−1969.01
Butene	11.4430	−1381.75

Note. $\ln p = A + B/T$.

Initial estimates were made for the sum of the liquid molar concentrations and for the values of Q_G, Q_L, and $C_{L,i}$. The objective function, OF (see below), was evaluated and then minimized using the optimization routine (4) by varying the values of Q_G, Q_L, and $C_{L,i}$. The optimization was terminated when the OF approached zero, rather than using the usual tests for optimization convergence, because the optimum point was the solution of three equations with three unknowns. Liquid molar concentrations determined by the model were used to derive improved solubility coefficients that were in turn used in further optimization routines until the solubilities converged. If the value of any of the parameters Q_G, Q_L, or $C_{L,i}$ were found to be negative, they were adjusted to a small positive value and a penalty added to the OF. The penalty (p) was proportional to the magnitude of the negative number and the proportional constant was chosen to affect the OF strongly, even if the parameter deviates only slightly below zero. It is stressed that such a penalty function does not affect the eventual solution of the model; it merely "dissuades" the optimization program from selecting negative values for the three parameters.

In this algorithm, nitrogen (as an inert, with $r_{N_2} = 0$) was taken into account using

$$C_{L,N_2} = \frac{F_{N_2}}{Q_G m_2 + Q_L}, \quad [27]$$

where

$$C_{L,2} = \frac{-b \pm \sqrt{b^2 - 4ac}}{2a},$$

where

$$\begin{aligned} a &= 2w_{cat}k_3 \\ b &= k_2 w_{cat} C_{L,1} + Q_G m_2 + Q_L \\ c &= -F_2 - k_1 w_{cat} C_{L,1}^2 \end{aligned} \quad [28]$$

$$C_{L,3} = \frac{k_2 w_{cat} C_{L,1} C_{L,2} + F_3}{k_2 w_{cat} C_{L,1} + Q_G m_3 + Q_L} \quad [29]$$

$$C_{L,4} = \frac{k_3 w_{cat} C_{L,2}^2 + k_2 w_{cat} C_{L,1} C_{L,3} + F_4}{k_2 w_{cat} C_{L,1} + Q_G m_4 + Q_L}. \quad [30]$$

Higher $C_{L,i}$ values were also calculated to take into consideration the effect of the term $Q_G m_i$. When m_i tended to zero, these terms (required only to calculate the sum of the concentrations $C_{L,i}$), could be calculated as a sum using Eq. [33] below:

$$C_{L,i} = \frac{k_2 w_{cat} C_{L,1} C_{L,i-1} + F_i}{k_2 w_{cat} C_{L,1} + Q_G m_i + Q_L} \quad [31]$$

$$\alpha = \frac{k_2 w_{cat} C_{L,1}}{k_2 w_{cat} C_{L,1} + Q_L} \quad [32]$$

$$\sum_{i=2}^{\infty} C_{L,i} = C_{L,2} + C_{L,3} + \cdots + C_{L,14} + \frac{1}{1-\alpha} C_{L,15} \quad [33]$$

$$r_1 = -2k_1 w_{cat} C_{L,1}^2 - k_2 w_{cat} C_{L,1} \sum_{i=2}^{\infty} C_{L,i} \quad [34]$$

$$\xi_1 = F_1 + r_1 - Q_G m_1 C_{L,i} - Q_L C_{L,i}. \quad [35]$$

From Eq. [23],

$$\sum_{i=1}^{\infty} i C_{L,i} = C_{L,1} + 2C_{L,2} + \cdots + 14C_{L,14} + 15_{L,15}\left[\frac{15}{1-\alpha} + \frac{\alpha}{(1-\alpha)^2}\right]. \quad [36]$$

Assuming that the liquid density of nitrogen equals that of the monomer,

$$\xi_2 = \frac{M_{N_2}}{M_1} C_{L,N_2} + \sum_{i=1}^{\infty} i C_{L,i} - \rho_L / M_1 \quad [37]$$

$$\xi_3 = M_{N_2} C_{L,N_2} + m_1 C_{L,1} + \cdots + m_{15} C_{L,15} - P/RT. \quad [38]$$

The OF was then calculated as the sum of the absolute values of the errors ξ,

$$0 = a_1|\xi_1| + a_2|\xi_2| + a_3|\xi_3| + p, \quad [39]$$

where a_1, a_2, and a_3 are constants, chosen so that each of the terms were of the same order of magnitude. This ensured that each of the terms exerts a comparable influence on the OF. The penalty function, p, of course has a much larger effect than any of the preceding terms should any of the parameters Q_C, Q_L, or $C_{L,i}$ become negative. Normally, $p = 0$.

5. RESULTS AND DISCUSSION

Product Distribution

Figure 4 shows a typical product spectrum obtained with ethene as feed in the slurry operations of the ethene oligomerization reaction using nickel-exchanged silica–alumina catalysts. The corresponding Schulz–Flory plot is depicted in Fig. 5. The effectiveness of the model in predicting the product distribution is clearly evident.

Rate Constants

The mathematical model assumes second-order kinetics for ethene oligomerization. The rate of consumption of ethene is dependent on both the rate of ethene dimerization and the rate of reaction between ethene and product oligomers. However, the rate of the dimerization dominates when ethene concentration is high because

- the rate constant for this process was higher and
- second-order kinetics were involved (Fig. 6).

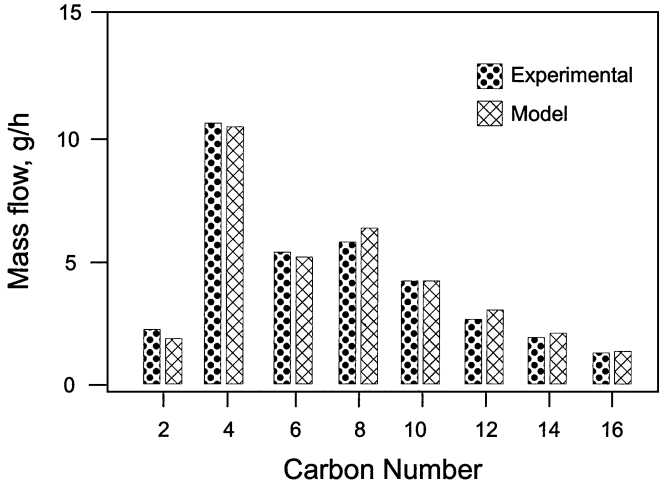

FIG. 4. Total product distribution (gas and liquid) by mass, for reaction at 160°C, MHSV = 3.9.

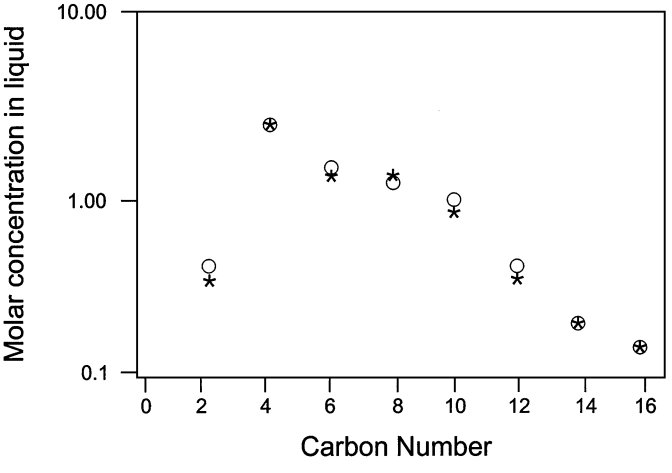

FIG. 5. Liquid-phase (molar) product distribution: ○, experimental; ✱, model.

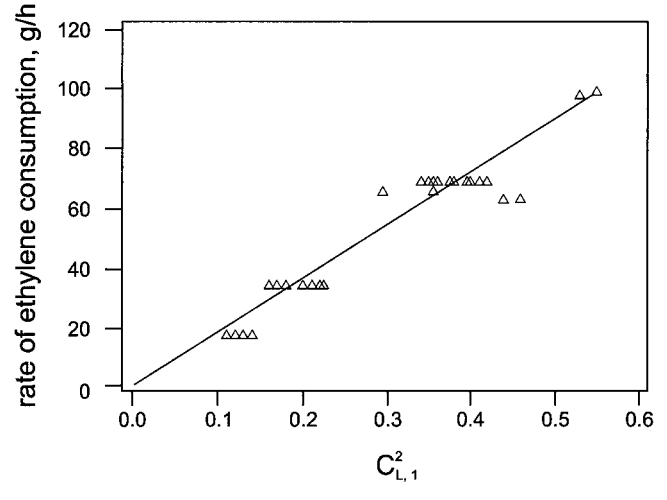

FIG. 6. Confirmation of the validity of second-order kinetics: △, experimental; —, model.

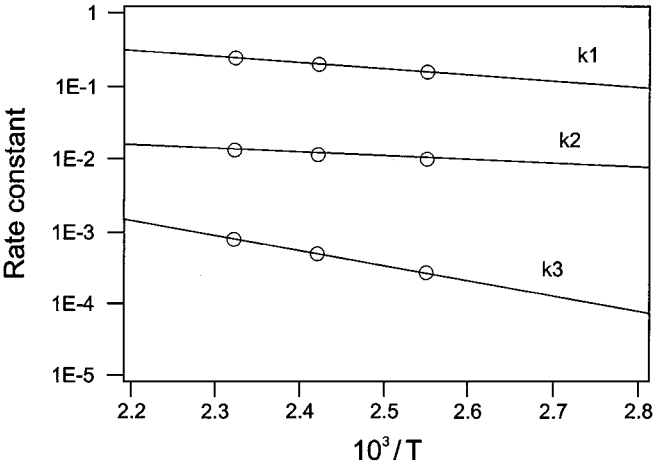

FIG. 7. Arrhenius plot for k_1, k_2, and k_3.

The temperature dependences of the three rate constants, k_1, k_2, and k_3 applicable to oligomerization with ethene as the feed, is shown in Fig. 7. Expressing the k values in terms of an Arrhenius expression:

$$k = A \exp(-E_a/RT).$$

The values of A and E_a were found as reported in Table 4.

Values of E_a for ethene–ethene (k_1) and ethene–oligomer (k_2) reactions are sufficiently close that they may reflect a similar activation step. The value of E_a (66.6 kJ mol^{-1}) associated with the butene–butene reaction (k_3) is very close to the value of 60 kJ mol^{-1} obtained for this reaction using butene in the continuous fixed-bed flow microreactor studies carried out with the identical catalysts (6). Since second-order kinetics were found for ethene oligomerization, and assuming that ethene adsorption–desorption equilibrium is reached, it is likely that the effective surface coverage of ethene in the present work is negligible. Consequently, the E_a values associated with k_1 and k_2 are likely to be apparent rather than real since the values obtained have been effectively lowered by an amount related to the enthalpy of adsorption of ethene on the catalyst. Butene is expected to have a lower enthalpy of adsorption than ethene, although we have no quantitative data to hand. The close similarity in E_a values obtained in this work and in the fixed-bed study (6) for butene are, however, encouraging and

TABLE 4

Rate Constants Used in the Model

	A (m^6 kg mol^{-1} h^{-1} kg_{cat}^{-1})	10^6A (m^6 kg mol^{-1} h^{-1} m_{cat}^{-2})	E_a (kJ mol^{-1})
k_1	20.1318	52.02	15.51
k_2	0.3485	0.9005	11.71
k_3	95320.0	246310	66.60

Note. $k = A \exp(-E_a/RT)$.

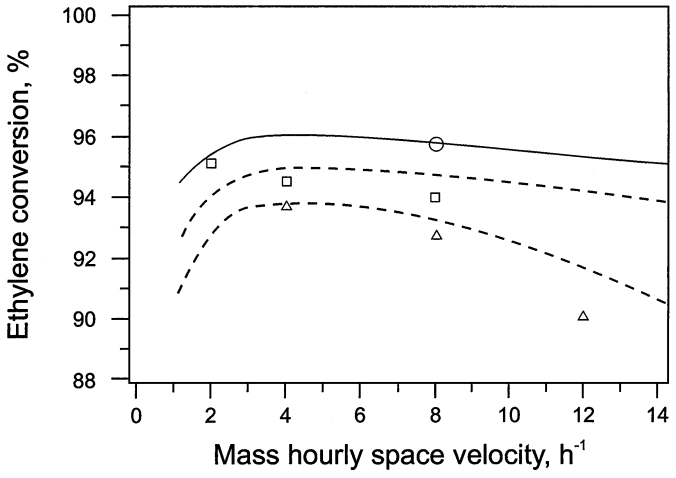

FIG. 8. Ethene conversion in the slurry reactor at various temperatures: ○, 120°C; □, 140°C; △, 160°C (experimental). —, 120°C; - - -, 140°C; · · ·, 160°C (model).

provide a strong element of consistency between the results secured from the two experimental systems. In addition, in the fixed-bed work, butene–butene dimerization (during ethene oligomerization) is clearly extensive, resulting in higher concentrations of octenes relative to those of the hexenes.

Conversion as a Function of Mass Hourly Space Velocity (MHSV)

Figure 8 depicts ethene conversion levels as a function of MHSV and reaction temperature, with experimental data and model predictions. The fall in conversion seen with increasing temperature in the range studied is in complete agreement with the observations made with ethene in fixed-bed microreactor work (1) where a pronounced fall in conversion was seen upon increasing the temperature of reaction from 120 to 160°C and attributed to the instability of the surface organometallic species, responsible for oligomerization, above a temperature of 120°C. In addition, the data fit the model fairly well, but for clarity some data have been omitted from Fig. 8. Some data were obtained for experimental nitrogen flow rates that differed somewhat from the value used in the model. In the model the nitrogen flow rate was assumed to be constant, while ethene flow was adjusted to change the MHSV. In some experiments, especially at lower values of MHSV, the nitrogen flow rate was also decreased. The correlation of all conditions tested with the model is given in Table 7. In this table, the model solution was obtained using the actual nitrogen flow rates used in the experiments.

Mass Transfer Limitations

Gas–liquid mass transfer limitations were assessed to be absent as a result of considering three criteria:

TABLE 5

Comparison of K ($= Y_i/X_i$) Values (See Text)

Component	With catalyst[a]	Without catalyst	
		Run 1	Run 2
Nitrogen	10.59 ± 1.44	11.21	11.34
Ethene	2.43 ± 0.34	2.85	2.97
Butene	0.772 ± 0.038	0.773	0.734
Hexene	0.240 ± 0.032	0.238	0.217
Octene	0.057 ± 0.011	0.139	0.065

[a] Ethene oligomerization at 120°C, 3.5 MPa, MHSV = 8.

(1) No effects on the observed kinetics were recorded for impeller speeds varying between 200 and 1500 rpm.

(2) Second-order kinetics remained valid, even at very high ethene concentrations, under which conditions the highest mass transfer rates are to be found.

(3) Special runs were conducted in the absence of a catalyst. A mixture was prepared that corresponded to that found experimentally under specific reaction conditions, namely, ethene feed, MHSV = 8, and reaction temperature = 120°C. This mixture was well stirred, and with the impeller stationary, a small amount of gas was analyzed as well as some liquid. Table 5 compares the average K values (y_i/x_i) of the active catalytic run with those obtained from two separate runs in which a catalyst was absent. The agreement between the sets of values is very good.

Finally, it was found that the model predictions of solubilities and the solubilities measured experimentally were in good agreement for a range of reaction temperatures with ethene fed at MHSV = 8 (Fig. 9).

The absence of intraparticle mass transfer limitations was demonstrated by varying the particle size range of the catalyst used. As shown in Table 6, the average particle size had

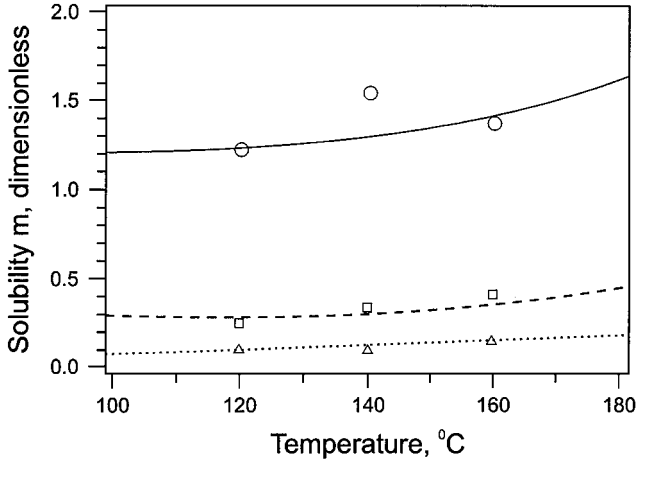

FIG. 9. Comparison of solubilities: ○, nitrogen; □, ethene; △, butene.

TABLE 6

Comparison of Rate Constants as a Function of Catalyst Particle Size

		Catalyst particle size (μm)		
		75–150	45–75 (run 1)	45–75 (run 2)
$10^6 k_1$	$m^6\ kg\ mol^{-1}\ h^{-1}\ kg_{cat}^{-1}$	0.2263 ± 0.0785	0.2138 ± 0.0539	0.1693 ± 0.0195
$10^6 k_1$	$m^6\ kg\ mol^{-1}\ h^{-1}\ km_{cat}^{-2}$	0.5848 ± 0.2029	0.5525 ± 0.1393	0.4375 ± 0.0504
$10^6 k_2$	$m^6\ kg\ mol^{-1}\ h^{-1}\ kg_{cat}^{-1}$	$1.15 \times 10^{-2} \pm 2.89 \times 10^{-3}$	$1.13 \times 10^{-2} \pm 1.40 \times 10^{-3}$	$9.25 \times 10^{-3} \pm 4.91 \times 10^{-4}$
$10^6 k_2$	$m^6\ kg\ mol^{-1}\ h^{-1}\ km_{cat}^{-2}$	$2.97 \times 10^{-2} \pm 7.5 \times 10^{-3}$	$2.92 \times 10^{-2} \pm 3.6 \times 10^{-3}$	$2.39 \times 10^{-2} \pm 1.3 \times 10^{-3}$

negligible effect on the kinetics of the reaction. Applying the Weisz criterion to the highest reaction rates measured using the largest particle diameters shows that diffusion effects may play a role. However, by using the fitted rate equations, it can be shown that, at all conditions, the effectiveness factor is always greater than 90%. This provides further evidence that the kinetics measured here are almost fully kinetically dominated and very insensitive to diffusion limitations. (In calculating the effectiveness factors porosity of 0.67 and catalyst density of 1250 kg m^{-3} were used.)

TABLE 7

Model Versus Measured Ethene Conversion

Temperature (°C)	MHSV	Conversion (model) (%)	Conversion (experimental) (%)	Difference (%)
120	8	95.6	95.6	0.0
140	1	97.6	95.8	1.8
140	2	94.7	95.2	−0.5
140	3	97.6	96.7	0.9
140	4	95.1	94.5	0.6
140	8	94.8	93.9	0.9
160	2	97.1	95.8	1.3
160	4	93.7	93.7	0.0
160	8	92.8	92.5	0.3
160	12	90.8	90.0	0.8

The maximum absolute rate of oligomerization of ethene found in this work exceeds 11.5 g g_{cat}^{-1} h^{-1}. (We have reason to believe that the nickel ion centres in these catalysts are essentially isolated (7) and on this basis this rate corresponds to a turnover frequency, TOF, of 0.42 s^{-1}.) Even higher rates may be expected from the extrapolation of data depicted in Fig. 8 since the percentage conversion falls only very slightly with increasing MHSV, particularly for a reaction temperature of 120°C. This finding, together with confirmation of the extremely low rates of deactivation seen in the present work, with no fall in activity apparent even after runs exceeding 900 h, once again demonstrates the high efficiency and stability of the nickel(II)-exchanged silica–alumina system and the present work provides adequate evidence for the practical application of the slurry reactor to effecting alkene oligomerization using this catalyst.

REFERENCES

1. Heveling, J., Nicolaides, C. P., and Scurrell, M. S., *Appl. Catal. A* **173**, 1 (1998).
2. Soave, G., *Chem. Eng. Sci.* **27**, 1197 (1972).
3. Flory, P. J., "Principles of Polymer Chemistry." Cornell Univ. Press, New York, 1953.
4. Caceci, M. S., and Cacheris, W. P., *Byte* 340 (1984).
5. Caldwell, L., and van Vuuren, D. S., private communication.
6. Nicolaides, C. P., and Scurrell, M. S., to be published.
7. Nicolaides, C. P., and Scurrell, M. S., presented at 4th Int. Symp. on Supported Reagents and Catalysts, St Andrews, July 2–6, 2000.